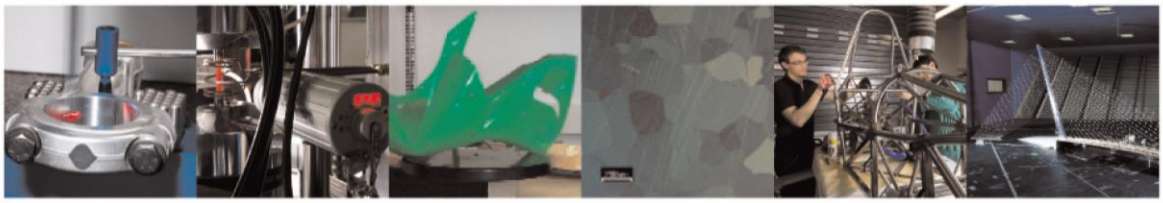

Hierarchical Metamodeling of the Air Bending Process

Strano, Matteo; Semeraro, Quirico; Iorio, Lorenzo; Sofia, Roberto

This is a post-peer-review, pre-copyedit version of an article published in JOURNAL OF MANUFACTURING SCIENCE AND ENGINEERING, 140/7, on May 21, 2018. The final authenticated version is available online at: http://dx.doi.org/10.1115/1.4040025

https://asmedigitalcollection.asme.org/manufacturingscience/article/doi/10.1115/1.4040025/473263/Hierarchical-Metamodeling-of-the-Air-Bending

DIPARTIMENTO DI MECCANICA ■ POLITECNICO DI MILANO
via G. La Masa, 1 ■ 20156 Milano ■ EMAIL (PEC): pecmecc@cert.polimi.it
http://www.mecc.polimi.it
Rev. 0

Hierarchical metamodeling of the air bending process

Matteo Strano[1]
Dipartimento di Meccanica, Politecnico di Milano
Via La Masa 1, 20156 Milan (Italy)
matteo.strano@polimi.it

Quirico Semeraro
Dipartimento di Meccanica, Politecnico di Milano
Via La Masa 1, 20156 Milan (Italy)
quirico.semeraro@polimi.it

Lorenzo Iorio
MUSP Lab
Str. della Torre della Razza, 29122 Piacenza (Italy)
lorenzo.iorio@polimi.it

Roberto Sofia
AMADA ENGINEERING EUROPE
Via Giovanni Agnelli, 15 – 10026 Santena (TO, Italy)
Roberto.Sofia@amada-engineering.eu

ABSTRACT

Despite the tremendous effort of researchers and manufacturing engineers in improving the predictability of the air bending process, there is still a strong need for comprehensive and dependable prediction models. Currently available modeling approaches all present some relevant limitations in practical applications. In this paper, we propose a new method, which represents an improvement over all existing modeling and prediction techniques. The proposed method can be used for accurate prediction of the main response variables of the air bending process: the angle α after springback and the bend deduction BD.

The metamodeling method is based on the hierarchical fusion of different kinds of data: the deterministic low-fidelity response of numerical FEM simulations and the stochastic high fidelity response of experimental tests. The metamodel has been built over a very large database,

[1] Corresponding author.

unprecedented in the scientific literature on air bending, made of more than 500 numerical simulations and nearly 300 experimental tests. The fusion is achieved first by interpolating the FEM simulations with a kriging predictor; then, the hierarchical metamodel is built as a linear regression model of the experimental data, using the kriging predictor among the regressors.

The accuracy of the method has been proved using a variant of the leave-one-out cross validation technique. The quality of the prediction yielded by the proposed method significantly over-performs the current prediction of the press brake on-line numerical control.

1. INTRODUCTION

From the point of view of the user, the angle α after springback and the bend deduction *BD* are the two most relevant responses of the air bending process. The bend deduction measures how much the flange length *L* of the sheet elongates after bending. These two process responses are largely determined by the geometry of the tools (the die width *w* and radius R_d, the punch radius R_p) and the blank material and thickness t_0. The most important geometrical variables of the air bending process are resumed in Fig. 1. With a given tooling and blank, the bend angles before (α_i) and after (α) springback can be varied by controlling the amount of vertical punch stroke, *s*. In the left part of Fig. 1, the punch is plotted at the beginning of its stroke (with a dotted line) and at the end of the stroke; the bend angle α_i before springback is shown. The sheet is also shown at the beginning of the process (with a dotted line) and at the end of the punch stroke. In the right part of Fig. 1 the geometry of the sheet after springback is shown.

An extensive literature is available on the prediction of air bending response variables, and especially on the prediction of the bend angle before α_i and after springback α. Despite the tremendous effort of researchers and manufacturing engineers in

improving the predictability of the air bending process [1], whenever a new sheet metal bent part is designed, both off-line CAD-based software [2] and on-line Numerical Controls (NC) of the press brakes [3] often fail to estimate the required amount of punch stroke *s* and the required initial length *L* of the sheet blank. Partly, this is because the air bending has an inherent, hardly reducible, process variability [4], i.e. it is affected by the blank-to-blank and batch-to-batch variability of material properties, sheet thickness, tribological conditions. As a consequence, setup adjustment runs are performed by the press brake operator in order to fine tune the air bending process [5]. In order to shorten or avoid these try-outs runs, press brake manufacturers have installed several on-line sensors and developed control algorithms, e.g. based on the on-line measurement of the bend angle [6] or the actual initial sheet thickness t_0 [7] or the punch force [8]. These on-line feedback controls are usually effective, but they increase the processing times [9] and they are often not appreciated by the users. Besides, these on-line process adjustments aim at finding the correct value of punch stroke *s* that yields a desired final bending angle α, but they can do little to control the amount of bend deduction *BD*, which is still an important outcome of the process. Besides, on-line feedback controls still require reliable prediction models of α in order to effectively compensate the punch stroke.

It can be concluded that, no matter how well equipped and how advanced is the press brake, there is still a strong need for comprehensive and dependable prediction models. In the scientific literature, five kinds of models can be found. For each type of model, only a few representative papers will be here cited for the sake of brevity.

1. Empirical or semi-empirical formulas [10] and practical rules [11], based on simplified modeling of the elastic-plastic deformation of the sheet metals. They

can only account for a few process variables, e.g. they are typically not able to account for anisotropy or friction. However, since the parameters of the empirical models are determined through experimental results and they can be included in look-up tables, these are the most widely used methods by industrial companies and press brake manufacturers. They fail whenever a new material comes into production. Industrially, the empirical prescriptions of the standard DIN 6935 are often implemented [12].

2. Experimental metamodels, such as statistical regression models [13] or metamodels based on artificial intelligence [14]. They can account for a larger base of process variables, they can often provide an estimation of uncertainty, but they have a very large model-building cost.
3. Complex theoretical models, based on the modeling of the elastic-plastic deformation of the sheet metals. These methods require finding numerical solutions to non-linear problems with short computational time. They can incorporate a relatively large amount of process variables. With very few exceptions [15], these models do not directly address the estimation of the variable of actual interest for the press users (e.g. the dependence of the final bending angle on the punch stroke). Furthermore, theoretical models always involve the estimation of the internal bending radius, which is a variable of scarce practical interest and very difficult to measure with accuracy.
4. FE (Finite Elements) methods, which are also based on modeling of the elastic-plastic deformation of the sheet metals; they are highly effective and reliable, but they require long computational times, hence they cannot be used for on-line purposes [16]. They could incorporate, virtually, all relevant process variables. FE

models sometimes fail to yield reliable results, especially because the air bending process is strongly influenced by the mechanics of springback, which is still one of the most difficult phenomena to be predicted by FEM.

5. Metamodels based on extensive campaigns of FEM simulations [17][18]. The meta-models obviously have a relatively large computational cost during the model-building phase, but they can be used on-line. They can incorporate virtually any model parameter and, unlike look-up tables, any parameter can be used continuously in its range, thanks to interpolation. Their predicting ability depends on the extension and the design of the underlying database of FE simulations [19] and, obviously, on the reliability of the FE simulation model itself.

In this paper a sixth, new type of method is proposed, based on the hierarchical metamodeling of both numerical FEM simulations and physical experiments. The proposed method overcomes most limitations of the alternative approaches: it allows fast on-line computation of the prediction, it reduces the numerical error of FE models because it corrects the numerical model with data of real experiments, it allows to consider all the relevant process variables.

The six above listed methods are summarized in Table 1, along with their main strengths and weaknesses.

Hierarchical metamodels, based on the fusion of experimental and numerical results, have been recently applied to sheet metal forming problems [20]. These metamodels are called hierarchical, because there is a hierarchy between different data sets: the results of physical experimental tests, though affected by measurement errors and scatter, are a direct representation of the process and are, therefore, high fidelity data

(hi-fi). Experimental data are stochastic in nature and they are usually available in a limited number, due to their high cost. Numerical results, i.e. the output of FEM simulations, are considered of low fidelity (lo-fi), but they are deterministic in nature.

The approach proposed in this paper is to build first a metamodel, built by interpolation over a large data base of numerical simulations, using a Kriging predictor. The kriging interpolator is then used as one of the variables of a statistical regression model, built over a large set of experimental conditions, replicated 2 or 3 times each. The logical flowchart of the proposed method is represented in Fig. 2, referred to a generic response variable *y*. The generic response *y* can be either the bend deduction *BD* or the bend angle α.

The paper is organized as follows: first the FEM model used for building the kriging interpolator is described (Section 2.1), along with the description of the numerical design space (Section 2.2), i.e. the input and output variables considered in the kriging metamodel. The kriging interpolation function of both response variables of interest (α and *BD*) is also presented (Section 2.3). In Section 3, the physical air bending experiments are described, including the experimental and measurement setups. In Section 4, the hierarchical metamodel is presented, and its robustness is verified by means of a demanding cross validation test.

2. FEM simulations and kriging metamodel

2.1 FEM simulation setup

The FEM simulation setup has been implemented with the commercial code Abaqus 6.14. The simulation model has been generated in 2D plane strain condition by

modelling the tools (punch and die) as discrete rigid bodies and the blank as a 2D planar deformable part (Fig. 3). The blank has been modelled with 8 node biquadratic plane strain quadrilateral elements with reduced integration (CPE8R). The mesh of the blank is finer at the center of the model, at the interface with the punch, with quadrilateral elements of 0.15 mm approximated edge length. Then the quadrilateral elements have been stretched along the x direction by considering a bias factor of 10 on 500 elements along the upper edge of the blank. The size of the elements varies between 5 and 15 elements through the thickness, increasing with the initial sheet thickness t_0. Thanks to a small computational cost of each FEM run, no symmetry plane has been used, so that the material in the region under the punch nose, where the maximum amount of deformation and springback takes place, is not over-constrained. The blank material has been defined with the elastic (Young's modulus and Poisson's ratio) and plastic properties (Yield stress / Plastic strain curve). The anisotropic material behaviour has been described by the classical Hill's anisotropic yield function. The coefficients F, G, H, L, M, N of the Hill's law are determined by the software itself, which requires as the user input the following values:

$$R_{11} = 1; R_{22} = \sqrt{\frac{r_y(r_x+1)}{r_x+r_y}}; R_{33} = \sqrt{\frac{r_y(r_x+1)}{r_x(r_y+1)}}; R_{12} = 1; R_{13} = \sqrt{\frac{3r_y(r_x+1)}{(2r_{xy}+1)(r_x+r_y)}}; R_{23} = 1$$

where the R_{ij} are the anisotropic yield stress ratios along the direction 1, 2 and 3 respectively defined in the model as X, Y and Z. The r_x, r_y and r_{xy} are the Lankford's anisotropic coefficients along the 0°, 90° and 45° rolling directions of the blank.

The simulation model is made in two steps:

- *Bending:* starting by the initial condition shown in Fig. 3a, the blank is bent by the descent of the punch with a velocity of 10 mm/s.

- *Springback:* the contacts between the blank and the tools are released and the blank recovers its elastic deformation. The isostatic condition is obtained by removing two degrees of freedom at two different nodes (Fig. 3b).

The objective of the simulation model was to obtain numerical estimates of the final opening angle (α_{FEM}) and the bend deduction (BD_{FEM}). A python script has been developed to extract the nodes coordinates of the blank extrados from the FEM model. The extrados nodal coordinates have been imported in a MATLAB script to calculate the bend angle, by fitting two segments along the straight portion of the right and left flanges. A general definition of *BD* is given in Fig. 4; it is obtained by subtracting the initial blank length L from the total length of the two flanges. The definition of *BD* changes if the final angle is lower or bigger than 90°, as shown in Fig. 4. A MATLAB script has been developed to calculate the final flange length considering the two different cases:

1. $\boldsymbol{\alpha_{FEM} \leq 90}$: the flange length FL_1 is calculated as the distance between the points with maximum and minimum abscissa. The operation is repeated for the second flange of the profile for measuring FL_2. The BD_{FEM} is calculated as:

$$BD_{FEM} = FL_1 + FL_2 - L \quad (1)$$

2. $\boldsymbol{\alpha_{FEM} > 90}$: three points are identified that define the flange lengths: the first and last nodes of the extrados, plus the intersection of the two straight tangent lines to the extrados. The BD_{FEM} values are obtained as in equation (1).

2.2 FEM design space

Using the FEM model described in the previous section, an extensive set of computer simulations has been run. The 13 input variables that vary in the FEM simulations are: the wall thickness t_0, 7 material properties, the tooling dimensions w (die opening), R_p

(punch nose radius), R_d (die corner radii), the punch stroke *s* and the Coulomb coefficient of friction *f*. In many models of air bending, the internal bend radius of the sheet R_i is also considered; however, it is not included in the numerical plan and will not be included in the experimental factors as well. The bend radius, unlike the sheet thickness, is not a design parameter, it is a consequence of the process. All the performed tests and simulations are "small radius" bending tests, i.e. they have been run with very small punch radius (0.8 mm). Therefore, the bending radius only depends on the geometry of the process (punch stroke, sheet thickness, die with) and it is strongly correlated to the bend angle. Besides, accurate measurement of the internal radius is rather difficult.

In the numerical data set, the estimation of the coefficient of friction is rather arbitrary, because it is a variable very difficult to be tuned and accurately assessed. The friction coefficient was selected in the typical range used in FEM simulation of sheet metal forming: e.g. 0.1 as a standard lubrication for steel-steel interface. In experiments, all friction conditions were constant, but some of the stainless steel samples were coated with a protection polymeric film. In simulation, this was assumed as a punch-sheet cof equal to 0.06.

The seven material variables are: the Young's modulus *E*, the yield strength R_s, the ratio R_m/R_s between tensile ad yield strengths, the elongation at fracture *A%*, the Lankford's normal anisotropy coefficient r_x in the bending direction, the Lankford's coefficient r_y and the average normal anisotropy r_{ave}. According to the orientation of the sheet, r_x can be either equal to the r_{90} material coefficient or the r_0. In the simulation, a 3-parameters hardening law for the flow stress $\bar{\sigma}$, as a function of the effective strain $\bar{\epsilon}$, has been used: $\bar{\sigma} = K(\epsilon_0 + \bar{\epsilon})^n$. Trivial mathematical relations have

been used to convert the engineering parameters R_s, R_m, $A\%$ to and from the hardening parameters K, ε_0 and n. The engineering parameters have been preferred in the design of computer simulations to be more familiar and more consistent with the engineering practice and with the material databases which are implemented in most NC controls of press brakes.

The 13 variables used in the plan of computer experiments are listed in Table 2, along with their investigated range. Space filling designs are the most commonly used for metamodeling of computer experiments [21]. In this case, we designed the simulations starting from a true space filling design, which was heavily modified for the following reasons:

- some geometrical variables are weakly correlated with each other (e.g. w with R_d), hence it makes no sense to test a condition where a very large w-value is used with a very small R_d value. all conditions which are not feasible or practical have been stripped from the initial plan.
- some material variables are correlated with each other (e.g. R_m>R_s) and are also bounded by physical or technological constraints; All conditions which are not feasible or practical have been stripped from the initial plan.

The initial space filling design was therefore cleaned from unfeasible or non realistic conditions. Besides, the design was modified by adding more runs:

- many FEM runs were conducted to simulate the physical experiments (see Section 3), which were designed under a different design of experiments;
- many FEM runs were added to the design, to replicate typical configurations, suggested by expert users of the press brake; in these additional runs, the

coefficient of friction was not varied randomly, but was kept fixed at either 0.06 or 0.1.

A complete graphical representation of the plan of FEM simulations is here too long to be reported, due to the very large number of variables and entries. As a mere example, in Fig. 5, 2 couples of design variables are shown: (t_0 and E), (r_x and r_{ave}). The variables of the first couple are completely independent on each other and the 2-D portion of the design space shown in Fig. 5a is uniformly filled. The two variables in the second couple are weakly correlated, hence the design space in Fig. 5b is not filled in the lower-right and upper-left regions. The final design of computer experiments includes 507 different simulation runs.

The results of all FEM simulations are summarised in Fig. 6, where the two main responses α_{FEM} and BD_{FEM} are plotted for each run. The figure shows the non-linear relation between these two responses, where larger values are obtained when α approaches 90°. Negative BD_{FEM} values can be obtained for very small bending angles, while the BD_{FEM} tends to zero when α_{FEM} approaches 180°.

2.3 Kriging metamodels

The typical approach used in the Design and Analysis of Computer Experiments (DACE) is to use a kriging model to approximate a deterministic computer model [22]. A kriging interpolator which performs a linear detrending [23] thanks to a linear regression has been used and it is described in this Section. First, the variables listed in table 2 have been transformed into a vector $\underline{x}$ of normalized variables of size p=13, with normalization in the range [0;1]. The FEM simulation has been repeated m=507 times, with m different values of the input vector $\underline{x}$. If y_{krig} is the generic kriging predictor, it expresses the deterministic response y_{FEM} (either BD_{FEM} or α_{FEM}) of the

FEM simulation for the input vector $\underline{x}$. y_{krig} is a realization of a regression model $F(\underline{x})$ and a correlation function $z(\underline{x})$:

$$y_{krig} = F(\underline{x}) + z(\underline{x}) = \beta_0 + \sum_{i=1}^{p} \beta_i \cdot f_i(\underline{x}) + z(\underline{x}) \quad (1)$$

where β_i is the i-th linear regression coefficient, $f_i(\underline{x})$ are the regression terms, each one is a function of a given input variable, $z(\underline{x})$ is a correlation function (stochastic process) with zero mean and covariance function:

$$cov[z(\underline{x}); z(\underline{w})] = \sigma^2 c(\theta, \underline{x}, \underline{w}) \quad (2)$$

where $\underline{x}$ and $\underline{w}$ are two distinct values of the input vector. c is a correlation function of $\underline{x}$ and $\underline{w}$ with a constant parameter θ. Computationally, the [m*p] matrix **S** of design points is available. Calculating the function c for each combination of rows of the data matrix **S**, a correlation matrix **C** is obtained. The parameter θ of the correlation function and the β_i coefficients are optimized in order to produce the following minimization:

$$\min_{\theta} |C|^{\frac{1}{m}} \sigma^2 \quad (3)$$

where **C** is the correlation matrix, $|C|$ is the determinant of **C**, m is the number of design points (507 in this case), σ^2 is also introduced in equation (2) and it is the maximum likelihood estimate of the process variance [24]. As the value of m increases, the minimization (3) becomes more and more similar to the simple minimization of σ^2.

This general formulation of the Kriging interpolation has been restricted with the following assumptions. Among many alternatives, the selected correlation function is

$$c(\theta, \underline{x}, \underline{w}) = \prod_{i=1}^{p} e^{-\theta \cdot |x_i - w_i|} \quad (4)$$

The function $c(\theta, \underline{x}, \underline{w})$ is exponentially decreasing with the distance between the values $\underline{x}$ and $\underline{w}$. A simple linear model $F(\underline{x})$ has been selected, using $f_i(\underline{x}) = x_i$. With the available data and the given assumptions, a kriging interpolator α_{krig} has been built according to equation (1), which yields a prediction of the angle α after springback. In the α_{krig} metamodel, the optimized value of the correlation parameter is θ=0.032, yielding σ= 39.85 °.

Another kriging interpolator has been built for yielding a prediction BD_{krig} of the bend deduction BD. The approach used for producing the BD_{krig} estimate is exactly the same described above. In the BD_{krig} metamodel, the optimized value of the correlation parameter is θ=0.150, yielding σ= 0.984 mm.

3. Air bending tests

3.1 Bending setup

The experimental activities have been performed in collaboration with Amada Engineering EU. The experimental tests were performed on an HG1003 press brake machine where the last version of numerical control (NC) software AMNC3i was installed. The AMNC3i has an integrated algorithm which allows to calculate the punch stroke by entering as inputs the material information and tools geometry from internal database, the thickness and the width of the blank, the target bend angle and the initial flange length. The calculated stroke *s* values have been used as input data not only in the tests, but also in the numerical FEM simulations which simulated the tests. The punch stroke values have been calculated by the software in order to reach a given "target" α-value. Four target angle values α_{NC} have been tested: 75°, 90°, 120° and

165°. The NC of the machines also yields an estimation of the expected bend deduction BD_{NC}. Five different materials have been tested: two types of steels, two types of stainless steels and one aluminum alloy. Tensile tests on all materials have been performed in order to obtain the mechanical properties.

The levels used for all experimental variables (material type and some geometrical parameters) are reported in Table 3. A full factorial design would require 2160 conditions, clearly too cumbersome. Only 108 conditions of the factors/levels listed in Table 3 have been selected by a factory expert. Each condition has been replicated 2 or 3 times, for a total number of 288 experimental results.

3.2 Measurement setup

The measurement activities have been performed in two phases. The measurements of the angle of the bent specimens have been performed with a digital goniometer. This allowed to reduce the measurement error within the interval of [-0.01; +0.01]°. The measurements of the specimens *BD* have been performed by taking in account the definition in Fig. 4. A specially designed measurement setup has been used to reduce the measurement error. In fact, in all sheet metal bending operations, the experimental measurement of the elongation of the fibers (or the measurement of the unlengthened) region is a critical and difficult task, even if using state of the art measuring techniques [25]. For specimens with final bend angle lower than or equal to 90°, a gauge block system has been implemented (Fig. 7) and a dial gauge has been used for measuring the flange lengths, within an accuracy close to 0.01 mm.

For specimens with final resulting angle α> 90°, a digital image acquisition and processing technique has been implemented. For the acquisition, a photographic setup has been built by using a reference plane, a NIKON D3300 camera positioned at

fixed focus distance and a controlled LED lighting system. In each photograph, the specimen and a standard component, previously measured with a micrometre, have been introduced to evaluate the scale (px/mm) to apply in the measurement phase. For the analysis, each photograph has been treated with ImageJ, with the integrated threshold Huang algorithm [26], in order to discretize and export the profile of the specimen (Fig. 8). ImageJ is a widely-used image processing program, designed for scientific use. The threshold level and method have been calibrated with the data coming from the previously mentioned mechanical BD measurement procedure. The profile of each specimen has been exported in Cartesian coordinates from each photograph. The analysis of the profile has been performed with a MATLAB® script.

3.3 Experimental results

The main purpose of the experimental plan is to generate the experimental hi-fi data, useful for building the hierarchical metamodeling. The large number of different tested experimental conditions (108), replicated to a total of 288 tests, will also allow to validate the model itself, by randomly splitting the experimental conditions into a training set and a verification set. A comprehensive report of the experimental results is out of the scope of this paper. Besides, the qualitative effect of the main process parameters and their sensitivity on the air bending results is well known to the users and has been investigated several times. However, it is interesting to evaluate the results in terms of errors. First, it must be noticed that the natural scatter of the data, measured trough the standard deviation, amount to 0.16° for the bending angle and to 0.09 mm for the BD. This means that no prediction model can ever reduce the average prediction error below these values. The difference, in absolute terms,

between the measured experimental angle values α and the target α_{NC} values can be measured as:

$$\varepsilon_{\alpha_{NC},i} = \left|\alpha_{NC,i} - \alpha_i\right| \qquad \forall\, i = 1,288 \tag{5}$$

Similarly, the absolute error on the prediction BD_{NC} of the bend deduction can be calculated:

$$\varepsilon_{BD_{NC},i} = \left|BD_{NC,i} - BD_i\right| \qquad \forall\, i = 1,288 \tag{6}$$

In Fig. 9, these absolute errors are grouped by target α levels. Larger absolute errors on *BD* are recorded for target angle α_{NC} =165°. Larger absolute errors on α are recorded for target angle α_{NC} =75°. The figure clearly explains why press brakes are often equipped with angle measurements sensors and controls and why process setup adjustments are required. Per Fig. 9, the typical error on the *BD* estimation is very frequently in excess of 0.2 mm and the typical error on the angle is very frequently in excess of 1°, i.e. outside the left-bottom box. These errors are unacceptable for most engineering applications, especially when consecutive bends are required on the same part. Besides, when the errors fall well outside the left-bottom box, it is not easy to adjust the process parameters to reach the required tolerances.

4. Hierarchical metamodel

4.1 Model building

The structure of the hierarchical metamodel is to merge, into a unique predictor, the information available from both the numerical and experimental results. Obviously, the validity of the proposed metamodel is restricted to the investigated range of parameters. The adopted approach is first explained with reference to the angle α. For the i-th experimentally measured value α_i, a discrepancy $\delta_{\alpha_i} = \left(\alpha_i - \alpha_{krig,i}\right)$ can

be calculated as the difference between the actual bending angle and its kriging prediction $\alpha_{krig,i}$. The δ_{α_i} values can be used for building a linear regression model:

$$\delta_{\alpha} = \alpha - \alpha_{krig} = \beta_0 + \sum_{j=1}^{N} \beta_j \cdot f_j(\underline{x}) + \varepsilon \quad (7)$$

where β_j are the regression coefficients, *N* is the number of regression functions $f_j(\underline{x})$ and ε is a white noise, i.e. a normally distributed statistical error with zero mean. A list of potential f_j functions to be included in the fusion regression model has been identified. The list includes:

- the 13 original independent terms listed in Table 2;
- 7 additional terms, presented in Table 5;
- all the first order interactions among the above listed 13+7 terms.

The 7 additional regression terms listed in Table 5 are: 3 functions of kriging predictors of angle and bend deduction (α_{krig}, $\beta_{krig}/2$, BD_{krig}); 2 functions which indicate the stiffness of the sheet material respectively in the elastic (K_{elas}) and the plastic (K_{plas}) regions; 3 empirical predictors of bending angle $\tilde{\alpha}$, punch stroke $\tilde{s}$ and internal bending radius R_i, which are sometimes used in the technical practice.

A stepwise heuristic algorithm has been used [27] for the selection of significant terms in the regression model, using a combined backward elimination and forward inclusion significance threshold of 0.0005. This routine allows selecting the best regression model, i.e. the best subset of regression terms out of the long list of potential terms, excluding all the terms with a significance level above 0.0005. The actual model selected by the stepwise algorithm includes N=13 regression functions for α. The resulting regression predictor $\hat{\delta}_{\alpha}$ can be considered a hierarchical metamodel, since it incorporates the kriging estimate α_{krig}:

$$\hat{\delta}_{\alpha} = \hat{\beta}_0 + \sum_{j=1}^{N} \hat{\beta}_j \cdot f_j(\underline{x}) \quad (8)$$

Once the $\hat{\delta}_{\alpha}$ model is available, the hierarchical metamodel prediction $\hat{\alpha}_i$ for each experimental run can finally be obtained as:

$$\hat{\alpha}_i = \hat{\delta}_{\alpha,i} + \alpha_{krig,i} \qquad \forall\, i = 1,288 \quad (9)$$

The same metamodeling approach has been implemented for the BD, obtaining a hierarchical metamodel $\widehat{BD}$ with only 8 terms.

The hierarchical metamodels $\hat{\alpha}$ and $\widehat{BD}$ have been calculated for all experimental points and the resulting absolute prediction errors can be calculated as:

$$\varepsilon_{\alpha_h,i} = |\hat{\alpha}_i - \alpha_i| \quad (10)$$

$$\varepsilon_{BD_h,i} = \left|\widehat{BD}_i - BD_i\right| \quad (11)$$

The plot of the absolute errors $\varepsilon_{\alpha_h,i}$ and $\varepsilon_{BD_h,i}$ is reported in Fig. 10 vs. the target α_{NC} (4 levels were planned in the experiments). The figure shows that the prediction error for the angle offered by the hierarchical metamodel is smaller at α_{NC}=165° than at the other target angles. The prediction error for the bend deduction is smaller at α_{NC}=75°. A comparison of Fig. 9 with Fig. 10 immediately shows how the hierarchical metamodel strongly improves the prediction offered by the press brake NC, since the cloud of points in Fig. 10 is much more concentrated near the origin of the plot space. In fact, in Fig. 10 the absolute error $\varepsilon_{\alpha_h,i}$ is always <2.5 °, and the absolute error $\varepsilon_{BD_h,i}$ is <0.45 mm. By comparison, the axes ranges in Fig. 9 are double as much. Besides, while in Fig. 9 four distinct clouds of points can be recognized, one for each target α_{NC} value, in Fig. 10 the four groups are mostly overlapped. This suggests that the absolute prediction error does not significantly depend on the target level of bend angle.

4.2 Cross validation

The two proposed metamodels $\hat{\alpha}$ and $\widehat{BD}$ are far from any physical interpretation of the process mechanics and, since they come from metamodeling of both computer and physical experiments, their validity is questionable not only outside the design space, but also in regions of the design space which have not been satisfactorily filled. For this reason, an experimental cross validation approach has been followed.

Before presenting the cross validation, it must be underlined that a purely experimental regression model for *y*, which does not incorporate the kriging predictor, has been built with the above described stepwise selection method. The resulting errors for both angle and bend deduction are statistically significantly larger than the errors of the hierarchical metamodels.

The approach is to estimate the β_j coefficients of both predictors $\hat{\delta}_\alpha$ and $\hat{\delta}_{BD}$ by using only a subset of the available 108 experimental conditions and the available 507 FEM runs. This subset is called the "training" set and it has been selected as a variant of the well-known leave-one-out cross validation methodology, typically used in regression models [28]. The purpose of this method is to compare each available experimental result $y_i(\underline{x})$ with metamodel predictions which have been built without the knowledge of both experimental y_i and numerical y_{FEM} results at that design point $\underline{x}$ and in its proximity.

The cross validation can be described as follows: let $\mathbf{X_{exp}}$ [108x13] and $\mathbf{X_{fem}}$ [507x13] be matrixes which define the full data sets of respectively 108 experimental conditions $\underline{x}$ and 507 numerical simulations. For each i^{th} row of $\mathbf{X_{exp}}$, i.e. for each experimental condition $\underline{x}_i$, a reduced matrix $\mathbf{X_{exp\_i}}$ [107x13] is created by stripping the i^{th} row. The minimum Euclidean distance of row $\underline{x}_i$ from all other rows of $\mathbf{X_{exp}}$ is calculated as d_{exp_i},

as a measure of proximity to the i^{th} design point. Then, a reduced $\mathbf{X_{fem\_i}}$ matrix is created by removing its rows which fall within a hypersphere centered in $\underline{x}_{exp\_i}$ and with radius $0.99 \cdot d_{exp\_i}$. At each iteration, this method leaves 1 experimental condition and 1 or 2 FEM simulation runs out of the design data sets. For each $\underline{x}_i$ condition, the kriging and the hierarchical models are recomputed using the same kriging and regression functions used for the full model of Section 4.1; then, the predictions $\hat{\alpha}_{red}$ and $\widehat{BD}_{red}$ are produced for the i-th condition with the reduced data sets. The resulting absolute errors $\varepsilon_{\alpha_{h\_red}}$ and $\varepsilon_{BD_{h\_red}}$ can be compared with the prediction errors of the numerical control $\varepsilon_{\alpha_{NC}}$ and $\varepsilon_{BD_{NC}}$. In Fig. 11, the boxplots of the absolute errors are shown. Graphically, there seems to be a superiority of the hierarchical metamodel, even if built with reduced datasets. Statistical analyses have been performed over the paired errors, in order to have a more objective response, and they uncontrovertibly confirmed that the hierarchical metamodels, developed only on the reduced data sets, outperform the NC prediction.

As a further cross validation test, the β_j coefficients of both predictors $\hat{\delta}_{\alpha}$ and $\hat{\delta}_{BD}$ have been calculated by using a training set with only 2/3 of the 108 available experimental conditions. Precisely, 34 experimental conditions with all their replicates have been randomly selected and stripped out of the available data. The 34 stripped conditions (amounting to 88 experimental runs because of the replicates) can be used as the "validation" set, i.e. the predictions $\hat{\alpha}_{red}$ and $\widehat{BD}_{red}$ can be produced on the validation design points. Again, the resulting absolute errors $\varepsilon_{\alpha_{h\_red}}$ and $\varepsilon_{BD_{h\_red}}$ can be compared with the prediction errors of the numerical control $\varepsilon_{\alpha_{NC}}$ and $\varepsilon_{BD_{NC}}$. The 88 calculated differences $\varepsilon_{\alpha\_h} - \varepsilon_{\alpha\_NC}$ have an average of -0.46°, i.e. the metamodel for the angle, although built only on 2/3 of the experimental points, still overperforms the NC

prediction. Similarly, the hierarchical metamodel for BD still overperforms the NC prediction by still 0.2 mm on average.

4.3 Discussion of results

The hierarchical metamodel, which combines the information coming from both experimental results and numerical simulations yields an improved accuracy if compared to a purely numerical kriging estimator or to a purely experimental regression predictor. In fact, If building a purely numerical kriging estimator, an unacceptable bias on the estimation of the experimental results would be obtained both for angle and bend deduction. If building a purely experimental regression model, solely based on the available experiments, the absolute $\varepsilon_{\alpha_h,i}$ would remain below 2.5°, but with a larger mean; the absolute error $\varepsilon_{BD_h,i}$ would be <1.2 mm, i.e. spread over a significantly larger range.

Furthermore, the cross validation of the model, presented in the previous Section, has shown that the proposed approach can lead to an improvement over the current prediction models implemented in industrial NC programs. The applicability of the models requires that the press brake software be equipped with a software able to handle, and to take as an input, the 13 input variables of the metamodel. Indeed, most of the 13 parameters are already currently implemented in the AMADA press brakes software, except for the 3 Lankford coefficients, which at the moment must be represented by a unique value of average normal anisotropy. The estimation of the coefficient of friction is critical, because it is a variable very difficult to be assessed, but the sensitivity of the metamodel with respect to f is limited. For every new material, new specific parameters should be introduced in the material DB, because it

would be impossible to obtain accurate predictions without accurate and reliable input data.

CONCLUSIONS

In this paper, we propose a new method for accurate prediction of the main response variables of the air bending process. The method can be used for calculating the angle α after springback for a given punch stroke, or it can be reversed for calculating the punch stroke for a target α. The method can also be used for calculating the bend deduction *BD*. The method is based on the hierarchical (fusion) metamodeling of a large number of both numerical FEM simulations and experimental results. The accuracy of the method has been tested against the current practice, by means of a severe cross-validation test, obtaining good results.

The proposed method overcomes all the limitations of all alternative approaches: it reduces the numerical error of FE models because it corrects the numerical model with data of real experiments; it allows to consider all the relevant process variables. Another crucial advantage of the proposed method is that provides a very fast computation of the prediction, thus allowing a potential on-line use.

In future applications of the developed model, the predictive ability of the developed metamodels could be continuously improved by adding new simulations and new experiments to the data sets.

As a further development, the hierarchical metamodeling will be applied to more complex air bending test cases, i.e. for modeling the geometry of simple components, such as u-shapes or hat-shapes, which are made as sequences of consecutive bends. In fact, the on-line tuning of air bending parameters is a much more lengthy and

difficult task when trying to control, at the same time, the angles and the flange lengths of consecutive bends.

FUNDING

This research has been partly funded by the project HIGH PERFORMANCE MANUFACTURING, code 4: CTN01_00163_216758, financed by the Italian Ministry of University and Research (MIUR), directed by prof. Michele Monno.

NOMENCLATURE

Symbol	description
A%	Elongation
α_i	initial bend angle, before springback, °
α	final bend angle, after springback, °
BD	bend deduction, mm
β_i	coefficient of a regression model
C	Correlation matrix of the of the kriging model
δ_y	difference between the actual response variable y and its kriging prediction y_{krig}
$\varepsilon_{y_h,i}$	absolute prediction error of the hierarchical metamodel at the *i-th* condition on any response variable *y*
$\varepsilon_{y_{NC},i}$	absolute prediction error of the numerical control at the *i-th* condition on any response variable *y*
f	Coulomb's coefficient of friction
$f_i(\underline{x})$	regression function in a linear regression model
FL	final flange length, mm
L	initial sheet length, mm
m	number of different FEM simulation runs, i.e. design points of the kriging metamodel
N	number of regression functions of the hierarchical metamodel
p	number of independent variables in FEM simulations
θ	parameter of the kriging correlation function

r_{ave}	average normal anisotropy coefficient
r_x, r_y and r_{xy}	Lankford's anisotropic coefficients along the 0°, 90° and 45° rolling directions
R_{ij}	anisotropic yield stress ratio along the direction i, j
R_d	die radius, mm
R_m	material ultimate tensile strenght, MPa
R_p	punch radius, mm
R_s	material yield strenght, MPa
s	punch stroke, mm
S	matrix of [m*n] design points in the kriging metamodel
t_0	sheet thickness, mm
w	die width or opening, mm
$\tilde{y}$	empirical estimate of any response variable y
$\hat{y}$	prediction of any response variable y yielded by a regression model
y_{FEM}	numerical FEM estimate of any response variable y
y_{krig}	kriging predictor of any response variable y
y_{NC}	target value of any response variable y, as predicted by the available numerical control of the press brake

REFERENCES

[1] Yang, X., Choi, C., Sever, N. K., and Altan, T., 2016, "Prediction of Springback in Air-Bending of Advanced High Strength Steel (DP780) Considering Young's Modulus Variation and with a Piecewise Hardening Function," Int. J. Mech. Sci., **105**, pp. 266–272.

[2] Kim, H., Nargundkar, N., and Altan, T., 2007, "Prediction of Bend Allowance and Springback in Air Bending," J. Manuf. Sci. Eng., **129**(2), pp. 342–351.

[3] Yang, M., Manabe, K.-I., and Nishimura, H., 1996, "Development of Real-Time Process Control System for Precision and Flexible V-Bending with an on-Line Database," J. Mater. Process. Technol., **60**, pp. 249–254.

[4] De Vin, L. J., 2000, "Curvature Prediction in Air Bending of Metal Sheet," J. Mater. Process. Technol., **100**(1–3), pp. 257–261.

[5] Wang, J., Verma, S., Alexander, R., and Gau, J.-T., 2008, "Springback Control of Sheet Metal Air Bending Process," J. Manuf. Process., **10**(1), pp. 21–27.

[6] De Vin, L. J., Streppel, A. H., Singh, U. P., and Kals, H. J. J., 1996, "A Process Model for Air Bending," J. Mater. Process. Technol., **57**, pp. 48–54.

[7] West, J. S., 1980, "Adaptive Stroke Reversal Control in Brakeforming," Massachusetts Institute of Technology.

[8] Kwok, S. K., and Lee, W. B., 1995, "The Development of a Machine Vision System for Adaptive Bending of Sheet Metals," J. Mater. Process. Technol., **48**(43–49).

[9] Elkins, K. L., and Sturges, R. H., 1999, "Springback Analysis and Control in Small Radius

Air Bending," J. Manuf. Sci. Eng., **121**, pp. 679–688.
[10] Raghupathi, P. S., Karima, M., Akgerman, N., and Altan, T., 1983, "A Simplified Approach to Calculate Springback in Brake Bending," *Proc. of NAMRC XI*, Madison (WI), pp. 165–170.
[11] Benson, S. D., 1997, *Press Brake Technology: A Guide to Precision Sheet Metal Bending*, Society of Manufacturing Engineers, Dearborn.
[12] 2011, *Cold Bending of Flat Rolled Steel*, DIN 6935:2011-10 (E).
[13] Gary Harlow, D., 2004, "The Effect of Statistical Variability in Material Properties on Springback," Int. J. Mater. Prod. Technol., **20**(1–3), pp. 180–192.
[14] Lin, Z.-C., Chang, D.-Y., 1996, "Application Model in of a Neural Network Machine Learning the Selection System of Sheet Metal Bending Tooling," Artif. Intell. Eng., **10**, pp. 21–37.
[15] Leu, D.-K., 1997, "A Simplified Approach for Evaluating Bendability and Springback in Plastic Bending of Anisotropic Sheet Metals," J. Mater. Process. Technol., **66**, pp. 9–17.
[16] Yilamu, K. et al., 2010, "Air Bending and Springback of Stainless Steel Clad Aluminum Sheet," J. Mater. Process. Technol., **210**(2), pp. 272–278.
[17] Wiebenga, J. H., Boogaard, a. H., and Klaseboer, G., 2012, "Sequential Robust Optimization of a V-Bending Process Using Numerical Simulations," Struct. Multidiscip. Optim., **46**(1), pp. 137–153.
[18] Hasser, P. J., Malik, A. S., Langer, K., Spradlin, T. J., and Hatamleh, M. I., 2016, "An Efficient Reliability-Based Simulation Method for Optimum Laser Peening Treatment," J. Manuf. Sci. Eng., **138**(11), p. 111001.
[19] Kennedy M, O., 2000, "Predicting the Output from a Complex Computer Code When Fast Approximations Are Available," Biometrika, **87**, pp. 1–13.
[20] Colosimo, B. M., Pagani, L., and Strano, M., 2015, "Reduction of Calibration Effort in FEM-Based Optimization via Numerical and Experimental Data Fusion," Struct. Multidiscip. Optim., **51**(2), pp. 463–478.
[21] Cioppa, T. M., and Lucas, T. W., 2007, "Efficient Nearly Orthogonal and Space-Filling Latin Hypercubes," Technometrics, **49**(1), pp. 45–55.
[22] Kleijnen, J. P. C., 2009, "Kriging Metamodeling in Simulation: A Review," Eur. J. Oper. Res., **192**(3), pp. 707–716.
[23] Martin, J. D., and Simpson, T. W., 2003, "A Study on the Use of Kriging Models to Approximate Deterministic Computer Models," *Volume 2: 29th Design Automation Conference, Parts A and B*, ASME, pp. 567–576.
[24] Simpson, T., Toropov, V., Balabanov, V., and Viana, F., 2008, "Design and Analysis of Computer Experiments in Multidisciplinary Design Optimization: A Review of How Far We Have Come - Or Not," *12th AIAA/ISSMO Multidisciplinary Analysis and Optimization Conference*, American Institute of Aeronautics and Astronautics, Reston, Virigina, pp. 1–22.
[25] Traub, T., and Groche, P., 2015, "Experimental and Numerical Determination of the Required Initial Sheet Width in Die Bending," Key Eng. Mater., **639**, pp. 147–154.
[26] Huang, Liang-Kai; Wang, M.-J. J., 1995, "Image Thresholding by Minimizing the Measures of Fuzziness," Pattern Recognit., **28**(1), pp. 41–51.
[27] Montgomery, Douglas C., Peck, E. A., and Vining, G. G., 2015, *Introduction to Linear Regression Analysis*, John Wiley & Sons.
[28] Krstajic, D., Buturovic, L. J., Leahy, D. E., and Thomas, S., 2014, "Cross-Validation Pitfalls When Selecting and Assessing Regression and Classification Models," J. Cheminform., **6**(1), p. 10.

Figure List

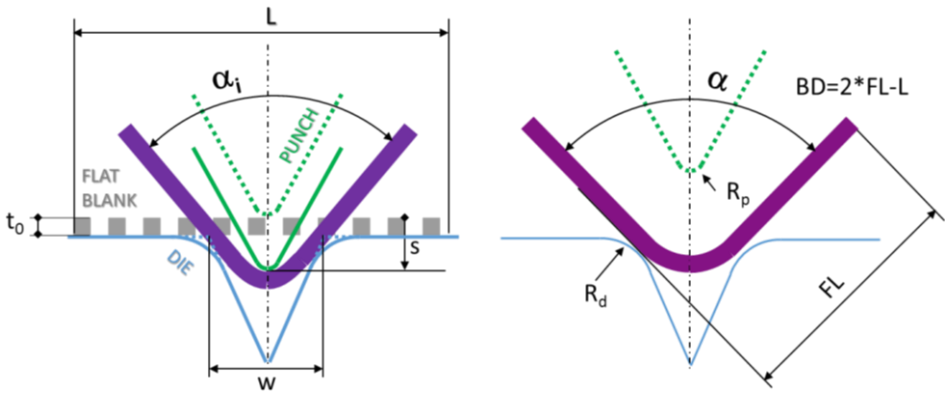

before punch stroke reversal *after springback*

Fig. 1: geometrical process parameters of air bending; the bend deduction BD is here defined under the assumption of a symmetric process and for a final angle $\alpha \leq 90°$.

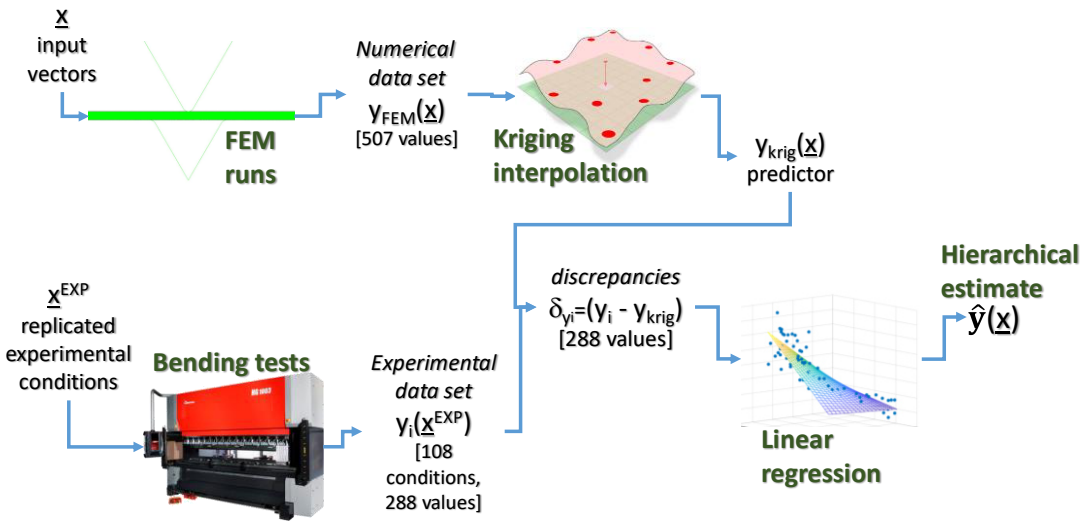

Fig. 2: logical flowchart of the proposed method for a generic response variable *y*.

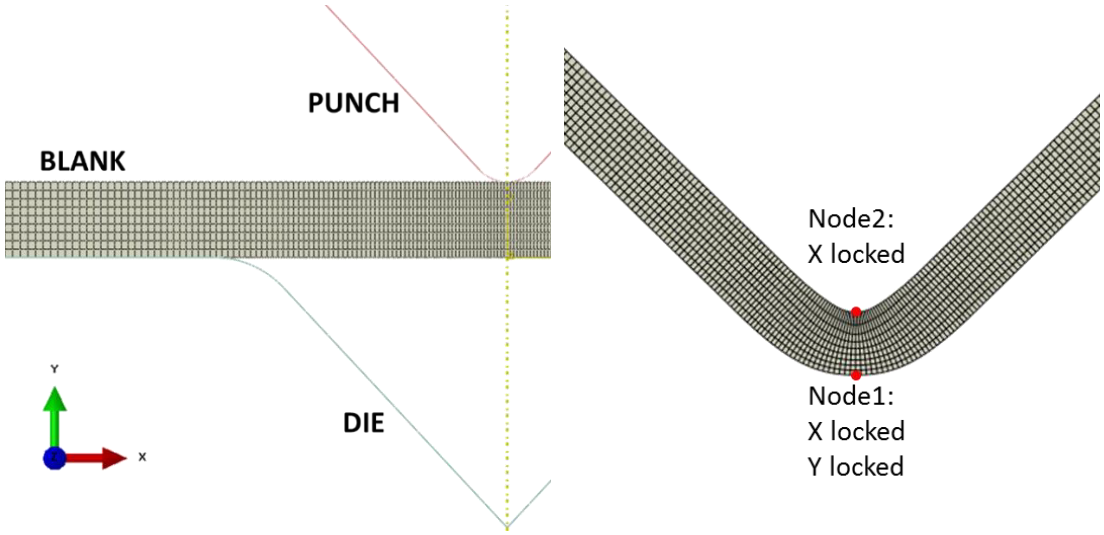

(a) (b)

Fig. 3: scheme of the simulation setup (a) and boundary conditions of the springback stage (b).

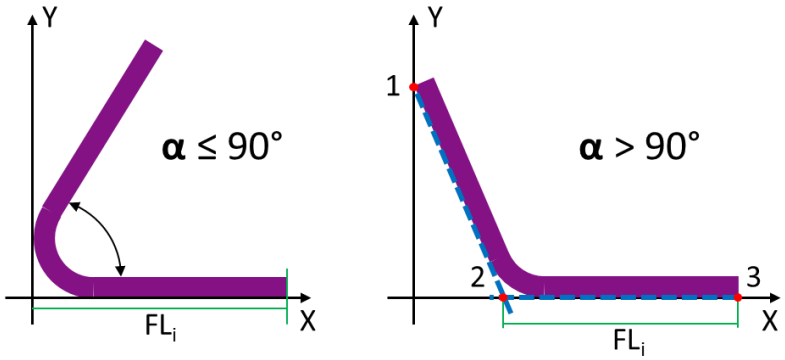

(a) (b)

Fig. 4: definition of the flange length from the standard DIN-6935 [12]; the initial sheet length is L, as defined in Fig. 1.

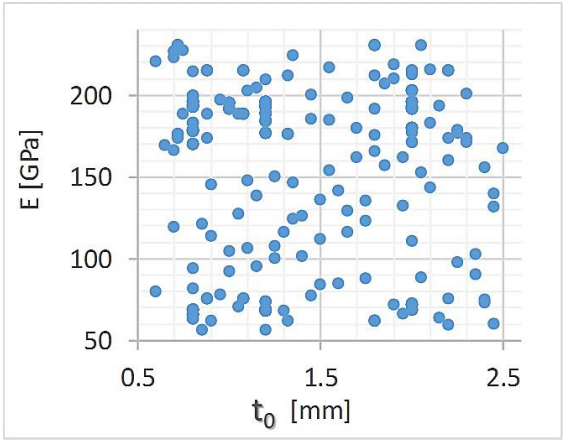

(a)

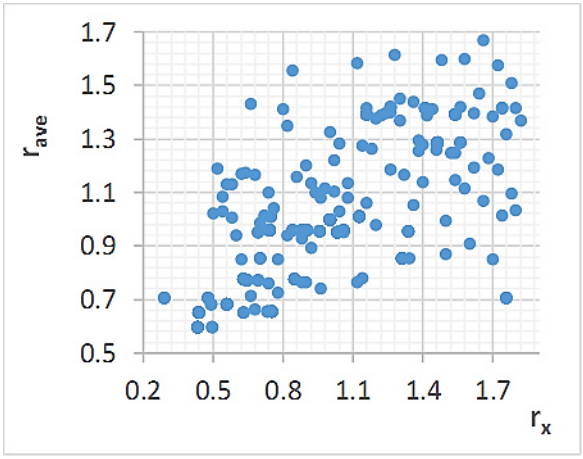

(b)

Fig. 5: two couples of variables tested in the FEM plan of simulations.

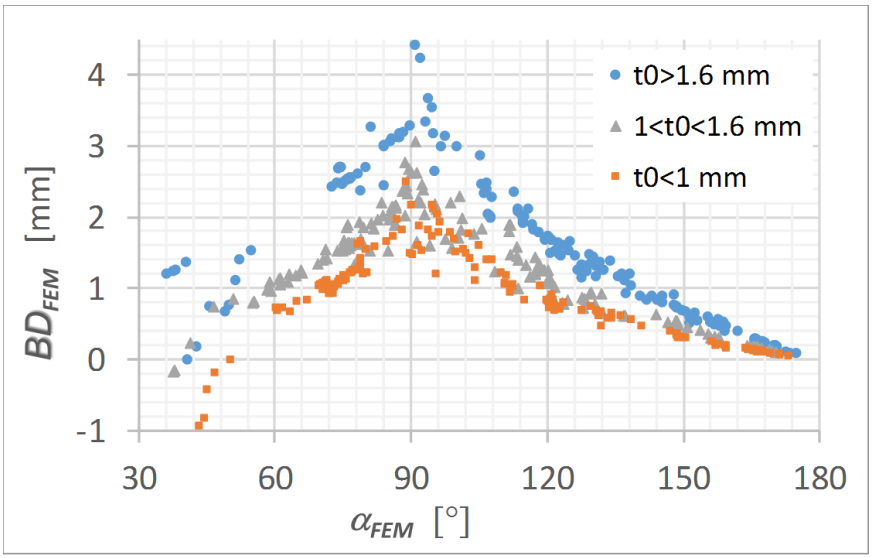

Fig. 6: plot of simulated BD_{FEM} vs α_{FEM}; data are grouped by levels of sheet thickness t_0.

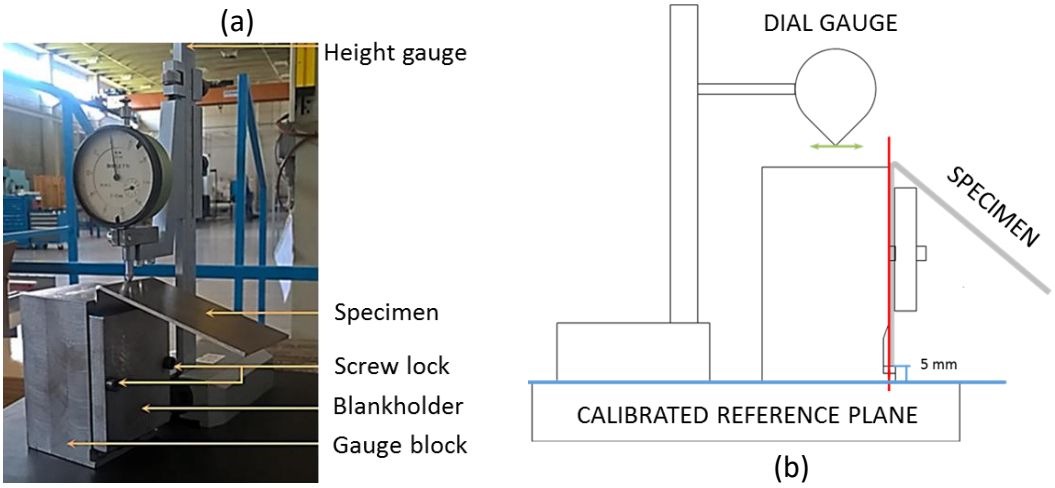

Fig. 7: experimental gauge block system (a), scheme of the flange length measurement (b).

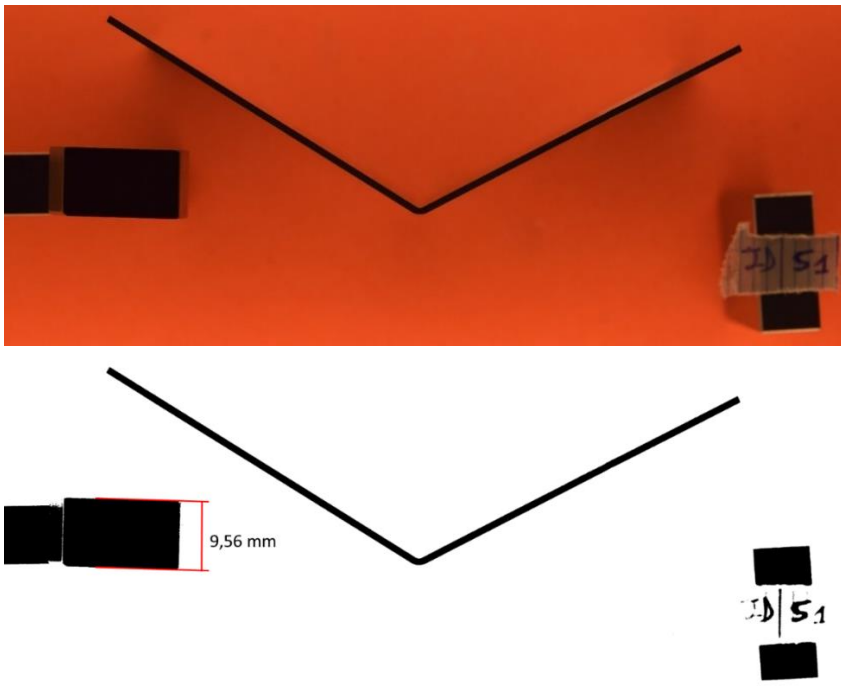

(a)

(b)

Fig. 8: photograph of specimen 51 (a), results of the threshold Huang algorithm (b).

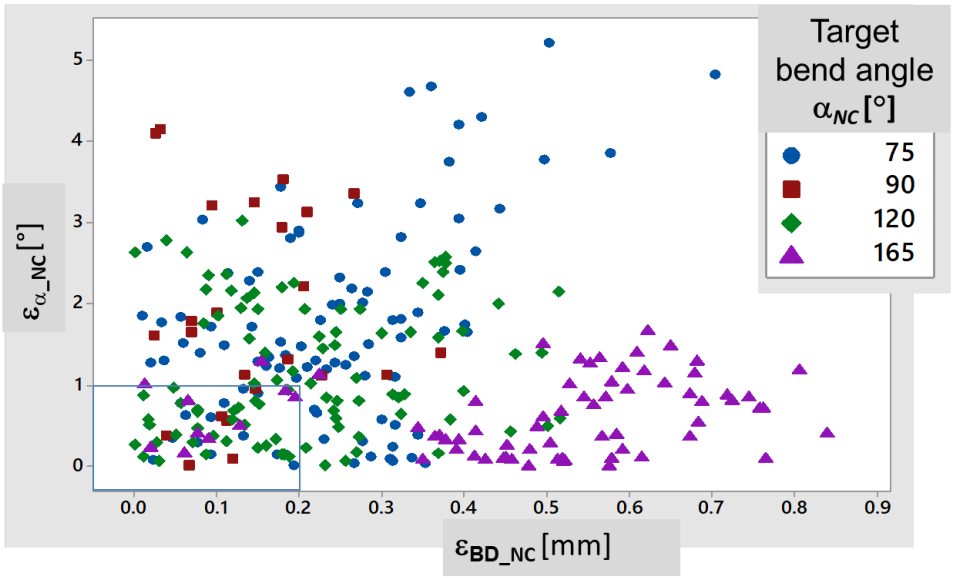

Fig. 9: absolute prediction errors $\varepsilon_{\alpha_{NC}}$ vs. $\varepsilon_{BD_{NC}}$ of the press brake; data are grouped by levels of target angle α_{NC}

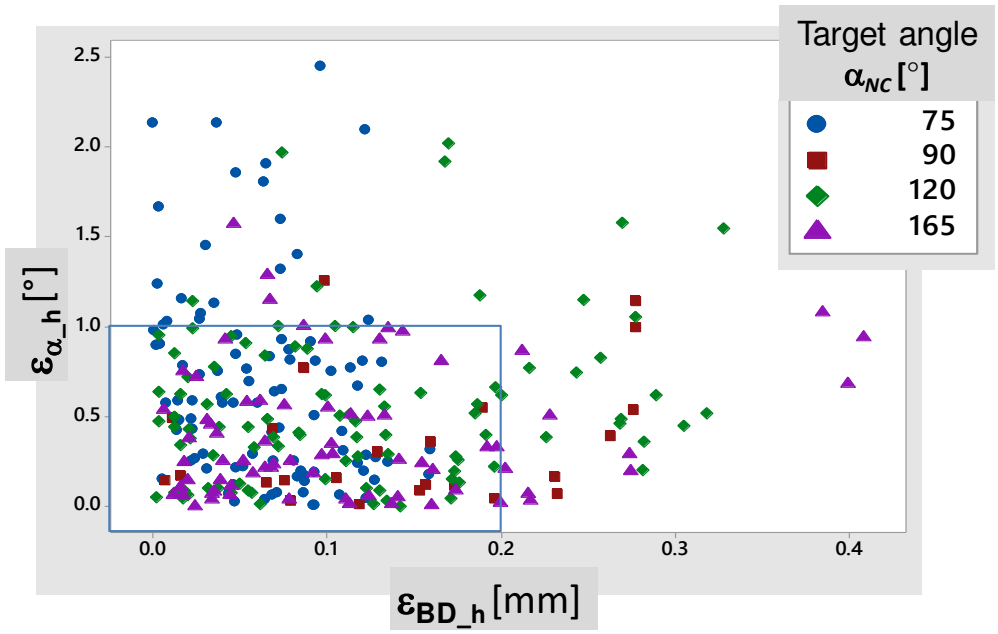

Fig. 10: absolute prediction errors ε_{α_h} vs. ε_{BD_h} of the hierarchical metamodels; data are grouped by levels of target angle α_{NC}.

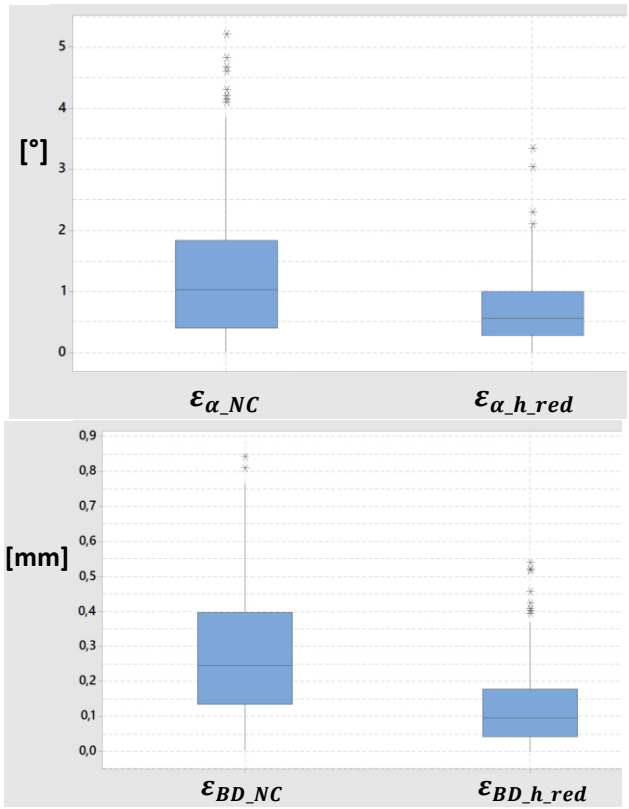

Fig. 11: boxplots of the absolute error differences for the angle (left) and the bend deduction (right); the hierarchical metamodels calculated over reduced data sets still overperform the NC prediction.

Table List

MODEL TYPOLOGY	STRENGTHS	WEAKNESSES
1. EMPIRICAL FORMULAS	Simplified modeling, robust to a wide range of each process variable, fast (allows on-line usage)	Inaccuracy, generally due to a reduced number of variables
2. EXPERIMENTAL METAMODELS	Accuracy	Large model-building cost, valid only in the experimental range
3. THEORETICAL MODELS	Short computational time, robust to a wide range of process variables	Not industrially relevant
4. FE METHODS	Account for many process variables (full elastic-plastic material behavior)	Long computational times
5. FEM-BASED METAMODELS	Account for many process variables, fast (allows on-line usage)	Not always accurate
6. HIERARCHICAL METAMODELS	Account for many process variables, fast (allows on-line usage), accurate	Depend on FEM plan dimension

Table 1: strengths and weakness of bending models listed previously.

Variable name and symbol		Unit	Min value	Max value
Wall thickness	t_0	(mm)	0.60	2.50
Young's modulus	E	(GPa)	56.7	231
Yield strength	R_s	(mPa)	36	545
Tensile vs. yield strength ratio	R_m/R_s		1.05	11.88
Elongation	$A\%$		0.12	0.70
Normal anisotropy coefficients	r_x		0.29	1.82
	r_y		0.29	1.82
	r_{ave}		0.60	1.67
Punch radius	R_p	(mm)	0.6	1.0
Die opening	w	(mm)	6.0	20.0
Die radius	R_d	(mm)	1.0	3.0
Punch stroke	s	(mm)	0.23	18.95
Coefficient of friction	f		0.061	0.180

Table 2: range of design parameters included in the FEM plan of computer experiments.

Factors		**Unit**	**Levels**				
Thickness	t_0	(mm)	0.8	1	1.2	2	
Punch radius	R_p	(mm)	0.60	0.65	0.80		
Die width	W	(mm)	6	8	10		
Die radius	R_d	(mm)	1.0	1.5	2.0		
Target bend angle	α_{NC}	(°)	75	90	120	165	
Material			FeP11	FeP06G	AISI304	AISI304 (D)	Al5754

Table 3: description of the factors investigated in the experimental activities.

name	Variable or function
Kriging predictors of bending angle and bend deduction	α_{krig}, BD_{krig}
Kriging estimate of half the external semi-angle $\beta/2$	$\frac{\beta_{krig}}{2} = \frac{(180 - \alpha_{krig})}{2}$
Material stiffness indicator in the elastic region	$K_{elas} = \frac{R_s}{E \cdot t_0}$
Material stiffness indicator in the plastic region	$K_{plas} = \frac{R_m \cdot A\%}{A\%^{A\%}}$
Empirical estimate of bending angle	$\tilde{\alpha} = arctan\left(\frac{w + {R_d}/{2}}{s - {R_p}/{5} - {t_0}/{5}}\right)$
Empirical estimate of punch stroke	$\tilde{s} = 0.5\left\{w \cdot tan\left(\frac{\beta_{krig}}{2}\right) + \left[1 - cos\left(\frac{\beta_{krig}}{2}\right) - tan\left(\frac{\beta_{krig}}{2}\right) \cdot sin\left(\frac{\beta_{krig}}{2}\right)\right](R_p + R_d + t_0)\right\}$
Empirical estimate of internal bending radius	$Ri = \frac{w \cdot tan\left(\frac{\beta_{krig}}{2}\right) + \frac{t_0}{2} - (\tilde{s} - t_0)}{sec\left(\frac{\beta_{krig}}{2}\right) - 1}$

Table 4: table of additional regressor functions f_j used in the forward-backward stepwise algorithm.